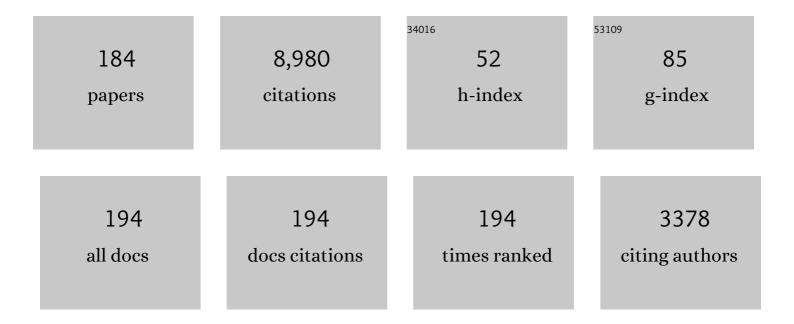
Eduard Y Chekmenev

List of Publications by Year in descending order

Source: https://exaly.com/author-pdf/6580628/publications.pdf

Version: 2024-02-01



#	Article	IF	CITATIONS
1	Analysis of Cancer Metabolism by Imaging Hyperpolarized Nuclei: Prospects for Translation to Clinical Research. Neoplasia, 2011, 13, 81-97.	2.3	623
2	Microtesla SABRE Enables 10% Nitrogen-15 Nuclear Spin Polarization. Journal of the American Chemical Society, 2015, 137, 1404-1407.	6.6	275
3	Parahydrogenâ€Based Hyperpolarization for Biomedicine. Angewandte Chemie - International Edition, 2018, 57, 11140-11162.	7.2	251
4	NMR Hyperpolarization Techniques for Biomedicine. Chemistry - A European Journal, 2015, 21, 3156-3166.	1.7	247
5	Towards hyperpolarized 13C-succinate imaging of brain cancer. Journal of Magnetic Resonance, 2007, 186, 150-155.	1.2	203
6	Near-unity nuclear polarization with an open-source ¹²⁹ Xe hyperpolarizer for NMR and MRI. Proceedings of the National Academy of Sciences of the United States of America, 2013, 110, 14150-14155.	3.3	193
7	Direct and cost-efficient hyperpolarization of long-lived nuclear spin states on universal ¹⁵ N ₂ -diazirine molecular tags. Science Advances, 2016, 2, e1501438.	4.7	193
8	¹⁵ N Hyperpolarization by Reversible Exchange Using SABRE-SHEATH. Journal of Physical Chemistry C, 2015, 119, 8786-8797.	1.5	192
9	Hyperpolarized NMR Spectroscopy: <i>d</i> â€DNP, PHIP, and SABRE Techniques. Chemistry - an Asian Journal, 2018, 13, 1857-1871.	1.7	180
10	Using low-E resonators to reduce RF heating in biological samples for static solid-state NMR up to 900MHz. Journal of Magnetic Resonance, 2007, 185, 77-93.	1.2	172
11	PASADENA Hyperpolarization of Succinic Acid for MRI and NMR Spectroscopy. Journal of the American Chemical Society, 2008, 130, 4212-4213.	6.6	170
12	LIGHT-SABRE enables efficient in-magnet catalytic hyperpolarization. Journal of Magnetic Resonance, 2014, 248, 23-26.	1.2	151
13	The Feasibility of Formation and Kinetics of NMR Signal Amplification by Reversible Exchange (SABRE) at High Magnetic Field (9.4 T). Journal of the American Chemical Society, 2014, 136, 3322-3325.	6.6	148
14	NMR Hyperpolarization Techniques of Gases. Chemistry - A European Journal, 2017, 23, 725-751.	1.7	140
15	Irreversible Catalyst Activation Enables Hyperpolarization and Water Solubility for NMR Signal Amplification by Reversible Exchange. Journal of Physical Chemistry B, 2014, 118, 13882-13889.	1.2	131
16	PASADENA hyperpolarization of 13C biomolecules: equipment design and installation. Magnetic Resonance Materials in Physics, Biology, and Medicine, 2009, 22, 111-121.	1.1	123
17	Over 20% ¹⁵ N Hyperpolarization in Under One Minute for Metronidazole, an Antibiotic and Hypoxia Probe. Journal of the American Chemical Society, 2016, 138, 8080-8083.	6.6	123
18	Parahydrogenâ€induced polarization (PHIP) hyperpolarized MR receptor imaging <i>in vivo</i> : a pilot study of ¹³ C imaging of atheroma in mice. NMR in Biomedicine, 2011, 24, 1023-1028.	1.6	116

#	Article	IF	CITATIONS
19	Generalizing, Extending, and Maximizing Nitrogen-15 Hyperpolarization Induced by Parahydrogen in Reversible Exchange. Journal of Physical Chemistry C, 2017, 121, 6626-6634.	1.5	112
20	¹⁵ N Hyperpolarization of Imidazole- ¹⁵ N ₂ for Magnetic Resonance pH Sensing via SABRE-SHEATH. ACS Sensors, 2016, 1, 640-644.	4.0	111
21	Quantitative Observation of Backbone Disorder in Native Elastin. Journal of Biological Chemistry, 2004, 279, 7982-7987.	1.6	104
22	Low-field MRI can be more sensitive than high-field MRI. Journal of Magnetic Resonance, 2013, 237, 169-174.	1.2	103
23	A pulsed injection parahydrogen generator and techniques for quantifying enrichment. Journal of Magnetic Resonance, 2012, 214, 258-262.	1.2	95
24	Heterogeneous Solution NMR Signal Amplification by Reversible Exchange. Angewandte Chemie - International Edition, 2014, 53, 7495-7498.	7.2	90
25	The Absence of Quadrupolar Nuclei Facilitates Efficient ¹³ C Hyperpolarization via Reversible Exchange with Parahydrogen. ChemPhysChem, 2017, 18, 1493-1498.	1.0	87
26	Hyperpolarization of "Neat―Liquids by NMR Signal Amplification by Reversible Exchange. Journal of Physical Chemistry Letters, 2015, 6, 1961-1967.	2.1	85
27	Open-Source Automated Parahydrogen Hyperpolarizer for Molecular Imaging Using ¹³ C Metabolic Contrast Agents. Analytical Chemistry, 2016, 88, 8279-8288.	3.2	84
28	Parahydrogen Induced Polarization of 1- ¹³ C-Phospholactate- <i>d</i> ₂ for Biomedical Imaging with >30,000,000-fold NMR Signal Enhancement in Water. Analytical Chemistry, 2014, 86, 5601-5605.	3.2	83
29	Direct Hyperpolarization of Nitrogen-15 in Aqueous Media with Parahydrogen in Reversible Exchange. Journal of the American Chemical Society, 2017, 139, 7761-7767.	6.6	80
30	Quality assurance of PASADENA hyperpolarization for 13C biomolecules. Magnetic Resonance Materials in Physics, Biology, and Medicine, 2009, 22, 123-134.	1.1	79
31	High-Resolution Structures and Orientations of Antimicrobial Peptides Piscidin 1 and Piscidin 3 in Fluid Bilayers Reveal Tilting, Kinking, and Bilayer Immersion. Journal of the American Chemical Society, 2014, 136, 3491-3504.	6.6	78
32	Hyperpolarized ¹ H NMR Employing Low γ Nucleus for Spin Polarization Storage. Journal of the American Chemical Society, 2009, 131, 3164-3165.	6.6	77
33	<i>In Situ</i> Detection of PHIP at 48 mT: Demonstration Using a Centrally Controlled Polarizer. Journal of the American Chemical Society, 2011, 133, 97-101.	6.6	75
34	A 3D-Printed High Power Nuclear Spin Polarizer. Journal of the American Chemical Society, 2014, 136, 1636-1642.	6.6	72
35	Highâ€Resolution 3D Proton MRI of Hyperpolarized Gas Enabled by Parahydrogen and Rh/TiO ₂ Heterogeneous Catalyst. Chemistry - A European Journal, 2014, 20, 11636-11639.	1.7	72
36	Propane- <i>d</i> ₆ Heterogeneously Hyperpolarized by Parahydrogen. Journal of Physical Chemistry C, 2014, 118, 28234-28243.	1.5	71

#	Article	IF	CITATIONS
37	PASADENA Hyperpolarized ¹³ C Phospholactate. Journal of the American Chemical Society, 2012, 134, 3957-3960.	6.6	70
38	Investigating molecular recognition and biological function at interfaces using piscidins, antimicrobial peptides from fish. Biochimica Et Biophysica Acta - Biomembranes, 2006, 1758, 1359-1372.	1.4	69
39	Facile Removal of Homogeneous SABRE Catalysts for Purifying Hyperpolarized Metronidazole, a Potential Hypoxia Sensor. Journal of Physical Chemistry C, 2018, 122, 16848-16852.	1.5	69
40	Longâ€Lived Spin States for Lowâ€Field Hyperpolarized Gas MRI. Chemistry - A European Journal, 2014, 20, 14629-14632.	1.7	65
41	Aqueous NMR Signal Enhancement by Reversible Exchange in a Single Step Using Water-Soluble Catalysts. Journal of Physical Chemistry C, 2016, 120, 12149-12156.	1.5	63
42	Long-Lived ¹³ C ₂ Nuclear Spin States Hyperpolarized by Parahydrogen in Reversible Exchange at Microtesla Fields. Journal of Physical Chemistry Letters, 2017, 8, 3008-3014.	2.1	63
43	Imaging amide proton transfer and nuclear overhauser enhancement using chemical exchange rotation transfer (CERT). Magnetic Resonance in Medicine, 2014, 72, 471-476.	1.9	62
44	Efficient Synthesis of Nicotinamide-1- ¹⁵ N for Ultrafast NMR Hyperpolarization Using Parahydrogen. Bioconjugate Chemistry, 2016, 27, 878-882.	1.8	62
45	Nanoscale Catalysts for NMR Signal Enhancement by Reversible Exchange. Journal of Physical Chemistry C, 2015, 119, 7525-7533.	1.5	61
46	In Situ and Ex Situ Lowâ€Field NMR Spectroscopy and MRI Endowed by SABRE Hyperpolarization. ChemPhysChem, 2014, 15, 4100-4107.	1.0	58
47	Heterogeneous Microtesla SABRE Enhancement of ¹⁵ N NMR Signals. Angewandte Chemie - International Edition, 2017, 56, 10433-10437.	7.2	58
48	XeNA: An automated â€~open-source' 129Xe hyperpolarizer for clinical use. Magnetic Resonance Imaging, 2014, 32, 541-550.	1.0	57
49	Toward Hyperpolarized ¹⁹ F Molecular Imaging via Reversible Exchange with Parahydrogen. ChemPhysChem, 2017, 18, 1961-1965.	1.0	57
50	Ion Solvation by Channel Carbonyls Characterized by 17O Solid-State NMR at 21 T. Journal of the American Chemical Society, 2005, 127, 11922-11923.	6.6	56
51	Parawasserstoffâ€basierte Hyperpolarisierung für die Biomedizin. Angewandte Chemie, 2018, 130, 11310-11333.	1.6	54
52	Ion-Binding Study by17O Solid-State NMR Spectroscopy in the Model Peptide Gly-Gly-Gly at 19.6 T. Journal of the American Chemical Society, 2006, 128, 9849-9855.	6.6	53
53	Efficient Synthesis of Molecular Precursors for Paraâ€Hydrogenâ€Induced Polarization of Ethyl Acetateâ€Iâ€≺sup>13C and Beyond. Angewandte Chemie - International Edition, 2016, 55, 6071-6074.	7.2	53
54	Instrumentation for Hydrogenative Parahydrogen-Based Hyperpolarization Techniques. Analytical Chemistry, 2022, 94, 479-502.	3.2	52

#	Article	IF	CITATIONS
55	Efficient Transformation of Parahydrogen Spin Order into Heteronuclear Magnetization. Journal of Physical Chemistry B, 2013, 117, 1219-1224.	1.2	51
56	Two-Dimensional Solid-State NMR Reveals Two Topologies of Sarcolipin in Oriented Lipid Bilayersâ€. Biochemistry, 2006, 45, 10939-10946.	1.2	48
57	Hyperpolarizing Concentrated Metronidazole ¹⁵ NO ₂ Group over Six Chemical Bonds with More than 15 % Polarization and a 20â€Minute Lifetime. Chemistry - A European Journal, 2019, 25, 8829-8836.	1.7	48
58	Spin Relays Enable Efficient Long-Range Heteronuclear Signal Amplification by Reversible Exchange. Journal of Physical Chemistry C, 2017, 121, 28425-28434.	1.5	46
59	Spin–Lattice Relaxation of Hyperpolarized Metronidazole in Signal Amplification by Reversible Exchange in Micro-Tesla Fields. Journal of Physical Chemistry C, 2018, 122, 4984-4996.	1.5	45
60	15N Chemical Shielding in Glycyl Tripeptides:Â Measurement by Solid-State NMR and Correlation with X-ray Structure. Journal of the American Chemical Society, 2004, 126, 379-384.	6.6	44
61	"Direct― ¹³ C Hyperpolarization of ¹³ Câ€Acetate by MicroTesla NMR Signal Amplification by Reversible Exchange (SABRE). Angewandte Chemie - International Edition, 2020, 59, 418-423.	7.2	41
62	Inhalable Curcumin: Offering the Potential for Translation to Imaging and Treatment of Alzheimer's Disease. Journal of Alzheimer's Disease, 2015, 44, 283-295.	1.2	40
63	Aqueous, Heterogeneous <i>para</i> -Hydrogen-Induced ¹⁵ N Polarization. Journal of Physical Chemistry C, 2017, 121, 15304-15309.	1.5	40
64	High-Field NMR Studies of Molecular Recognition and Structureâ^'Function Relationships in Antimicrobial Piscidins at the Waterâ^'Lipid Bilayer Interface. Journal of the American Chemical Society, 2006, 128, 5308-5309.	6.6	39
65	Low-E probe for 19F–1H NMR of dilute biological solids. Journal of Magnetic Resonance, 2007, 189, 182-189.	1.2	39
66	High-Resolution Low-Field Molecular Magnetic Resonance Imaging of Hyperpolarized Liquids. Analytical Chemistry, 2014, 86, 9042-9049.	3.2	39
67	Temperature Cycling Enables Efficient ¹³ C SABRE-SHEATH Hyperpolarization and Imaging of [1- ¹³ C]-Pyruvate. Journal of the American Chemical Society, 2022, 144, 282-287.	6.6	39
68	Temperature-Ramped ¹²⁹ Xe Spin-Exchange Optical Pumping. Analytical Chemistry, 2014, 86, 8206-8212.	3.2	37
69	Flow-Through Lipid Nanotube Arrays for Structure-Function Studies of Membrane Proteins by Solid-State NMR Spectroscopy. Biophysical Journal, 2006, 91, 3076-3084.	0.2	36
70	Production of Pure Aqueous ¹³ Câ€Hyperpolarized Acetate by Heterogeneous Parahydrogenâ€Induced Polarization. Chemistry - A European Journal, 2016, 22, 16446-16449.	1.7	36
71	NMR Spin-Lock Induced Crossing (SLIC) dispersion and long-lived spin states of gaseous propane at low magnetic field (0.05 T). Journal of Magnetic Resonance, 2017, 276, 78-85.	1.2	36
72	Unveiling coherentlyÂdriven hyperpolarization dynamics in signal amplification by reversible exchange. Nature Communications, 2019, 10, 395.	5.8	36

#	Article	IF	CITATIONS
73	Quasi-Resonance Signal Amplification by Reversible Exchange. Journal of Physical Chemistry Letters, 2018, 9, 6136-6142.	2.1	35
74	Single-Crystal Studies of Peptide Prolyl and Glycyl15N Shielding Tensors. Journal of the American Chemical Society, 2005, 127, 9030-9035.	6.6	34
75	Sodium MRI in a rat migraine model and a NEURON simulation study support a role for sodium in migraine. Cephalalgia, 2011, 31, 1254-1265.	1.8	34
76	NMR Signal Amplification by Reversible Exchange of Sulfurâ€Heterocyclic Compounds Found In Petroleum. ChemistrySelect, 2016, 1, 2552-2555.	0.7	34
77	17O Quadrupole Coupling and Chemical Shielding Tensors in an H-bonded Carboxyl Group:  α-Oxalic Acid. Journal of the American Chemical Society, 2003, 125, 9140-9146.	6.6	33
78	Analysis of RF heating and sample stability in aligned static solid-state NMR spectroscopy. Journal of Magnetic Resonance, 2006, 180, 51-57.	1.2	33
79	A large volume flat coil probe for oriented membrane proteins. Journal of Magnetic Resonance, 2006, 181, 9-20.	1.2	33
80	MR Imaging Biomarkers in Oncology Clinical Trials. Magnetic Resonance Imaging Clinics of North America, 2016, 24, 11-29.	0.6	33
81	Chemical Exchange Reaction Effect on Polarization Transfer Efficiency in SLIC-SABRE. Journal of Physical Chemistry A, 2018, 122, 9107-9114.	1.1	33
82	Synthesis of Unsaturated Precursors for Parahydrogen-Induced Polarization and Molecular Imaging of 1- ¹³ C-Acetates and 1- ¹³ C-Pyruvates via Side Arm Hydrogenation. ACS Omega, 2018, 3, 6673-6682.	1.6	33
83	¹⁵ N MRI of SLICâ€SABRE Hyperpolarized ¹⁵ Nâ€Labelled Pyridine and Nicotinamide. Chemistry - A European Journal, 2019, 25, 8465-8470.	1.7	33
84	¹⁵ N NMR Hyperpolarization of Radiosensitizing Antibiotic Nimorazole by Reversible Parahydrogen Exchange in Microtesla Magnetic Fields. Angewandte Chemie - International Edition, 2021, 60, 2406-2413.	7.2	33
85	15N and 31P solid-state NMR study of transmembrane domain alignment of M2 protein of influenza A virus in hydrated cylindrical lipid bilayers confined to anodic aluminum oxide nanopores. Journal of Magnetic Resonance, 2005, 173, 322-327.	1.2	32
86	Multidimensional Mapping of Spin-Exchange Optical Pumping in Clinical-Scale Batch-Mode 129Xe Hyperpolarizers. Journal of Physical Chemistry B, 2014, 118, 4809-4816.	1.2	32
87	Quantifying the effects of quadrupolar sinks <i>via</i> ¹⁵ N relaxation dynamics in metronidazoles hyperpolarized <i>via</i> SABRE-SHEATH. Chemical Communications, 2020, 56, 9098-9101.	2.2	32
88	Functional stability of water wire–carbonyl interactions in an ion channel. Proceedings of the National Academy of Sciences of the United States of America, 2020, 117, 11908-11915.	3.3	32
89	2D Mapping of NMR Signal Enhancement and Relaxation for Heterogeneously Hyperpolarized Propane Gas. Journal of Physical Chemistry C, 2017, 121, 10038-10046.	1.5	31
90	Orderâ€Unity ¹³ C Nuclear Polarization of [1â€ ¹³ C]Pyruvate in Seconds and the Interplay of Water and SABRE Enhancement. ChemPhysChem, 2022, 23, .	1.0	30

#	Article	IF	CITATIONS
91	Peptide17O Chemical Shielding and Electric Field Gradient Tensors. Journal of Physical Chemistry B, 2006, 110, 22935-22941.	1.2	29
92	Toward production of pure ¹³ C hyperpolarized metabolites using heterogeneous parahydrogen-induced polarization of ethyl[1- ¹³ C]acetate. RSC Advances, 2016, 6, 69728-69732.	1.7	28
93	Parahydrogen-Induced Polarization of 1- ¹³ C-Acetates and 1- ¹³ C-Pyruvates Using Sidearm Hydrogenation of Vinyl, Allyl, and Propargyl Esters. Journal of Physical Chemistry C, 2019, 123, 12827-12840.	1.5	28
94	Pulse-Programmable Magnetic Field Sweeping of Parahydrogen-Induced Polarization by Side Arm Hydrogenation. Analytical Chemistry, 2020, 92, 1340-1345.	3.2	28
95	Fluorine-19 NMR Chemical Shift Probes Molecular Binding to Lipid Membranes. Journal of Physical Chemistry B, 2008, 112, 6285-6287.	1.2	27
96	A large volume double channel 1H–X RF probe for hyperpolarized magnetic resonance at 0.0475T. Journal of Magnetic Resonance, 2012, 220, 94-101.	1.2	27
97	Demonstration of Heterogeneous Parahydrogen Induced Polarization Using Hyperpolarized Agent Migration from Dissolved Rh(I) Complex to Gas Phase. Analytical Chemistry, 2014, 86, 6192-6196.	3.2	27
98	Robust Imidazoleâ€ ¹⁵ N ₂ Synthesis for Highâ€Resolution Lowâ€Field (0.05 T) ¹⁵ NÂHyperpolarized NMR Spectroscopy. ChemistrySelect, 2017, 2, 4478-4483.	0.7	27
99	Heterogeneous Microtesla SABRE Enhancement of ¹⁵ N NMR Signals. Angewandte Chemie, 2017, 129, 10569-10573.	1.6	27
100	Parahydrogenâ€Induced Hyperpolarization of Gases. Angewandte Chemie - International Edition, 2020, 59, 17788-17797.	7.2	27
101	Clinical-Scale Production of Nearly Pure (>98.5%) Parahydrogen and Quantification by Benchtop NMR Spectroscopy. Analytical Chemistry, 2021, 93, 3594-3601.	3.2	27
102	Dephosphorylation and biodistribution of 1â€ ¹³ Câ€phospholactate <i>in vivo</i> . Journal of Labelled Compounds and Radiopharmaceuticals, 2014, 57, 517-524.	0.5	26
103	High-resolution hyperpolarized in vivo metabolic 13C spectroscopy at low magnetic field (48.7 mT) following murine tail-vein injection. Journal of Magnetic Resonance, 2017, 281, 246-252.	1.2	26
104	Enabling Clinical Technologies for Hyperpolarized ¹²⁹ Xenon Magnetic Resonance Imaging and Spectroscopy. Angewandte Chemie - International Edition, 2021, 60, 22126-22147.	7.2	26
105	Parahydrogen-Induced Polarization with a Rh-Based Monodentate Ligand in Water. Journal of Physical Chemistry Letters, 2012, 3, 3281-3285.	2.1	25
106	Imaging of Biomolecular NMR Signals Amplified by Reversible Exchange with Parahydrogen Inside an MRI Scanner. Journal of Physical Chemistry C, 2017, 121, 25994-25999.	1.5	25
107	A pulse programmable parahydrogen polarizer using a tunable electromagnet and dual channel NMR spectrometer. Journal of Magnetic Resonance, 2017, 284, 115-124.	1.2	24
108	Glycyl CαChemical Shielding in Tripeptides: Measurement by Solid-State NMR and Correlation with X-ray Structure and Theory. Journal of the American Chemical Society, 2002, 124, 11894-11899.	6.6	23

#	Article	IF	CITATIONS
109	¹⁹ F Hyperpolarization of ¹⁵ N-3- ¹⁹ F-Pyridine via Signal Amplification by Reversible Exchange. Journal of Physical Chemistry C, 2018, 122, 23002-23010.	1.5	23
110	Quasi-Resonance Fluorine-19 Signal Amplification by Reversible Exchange. Journal of Physical Chemistry Letters, 2019, 10, 4229-4236.	2.1	23
111	Clinical-Scale Batch-Mode Production of Hyperpolarized Propane Gas for MRI. Analytical Chemistry, 2019, 91, 4741-4746.	3.2	23
112	Rational ligand choice extends the SABRE substrate scope. Chemical Communications, 2020, 56, 9336-9339.	2.2	23
113	Subâ€second proton imaging of ¹³ C hyperpolarized contrast agents in water. Contrast Media and Molecular Imaging, 2014, 9, 333-341.	0.4	22
114	Parahydrogenâ€Induced Radio Amplification by Stimulated Emission of Radiation. Angewandte Chemie - International Edition, 2020, 59, 8654-8660.	7.2	22
115	Can antimicrobial peptides scavenge around a cell in less than a second?. Biochimica Et Biophysica Acta - Biomembranes, 2010, 1798, 228-234.	1.4	21
116	NMR SLIC Sensing of Hydrogenation Reactions Using Parahydrogen in Low Magnetic Fields. Journal of Physical Chemistry C, 2016, 120, 29098-29106.	1.5	21
117	Gas Phase UTE MRI of Propane and Propene. Tomography, 2016, 2, 49-55.	0.8	21
118	Synthesis and physico-chemical properties of peptides in soil humic substances. Chemical Biology and Drug Design, 2004, 63, 253-264.	1.2	20
119	Current and emerging quantitative magnetic resonance imaging methods for assessing and predicting the response of breast cancer to neoadjuvant therapy. Breast Cancer: Targets and Therapy, 2012, 2012, 139.	1.0	20
120	Low-Cost High-Pressure Clinical-Scale 50% Parahydrogen Generator Using Liquid Nitrogen at 77 K. Analytical Chemistry, 2021, 93, 8476-8483.	3.2	20
121	Heterogeneous Parahydrogen Pairwise Addition to Cyclopropane. ChemPhysChem, 2018, 19, 2621-2626.	1.0	19
122	Batch-Mode Clinical-Scale Optical Hyperpolarization of Xenon-129 Using an Aluminum Jacket with Rapid Temperature Ramping. Analytical Chemistry, 2020, 92, 4309-4316.	3.2	19
123	SABRE and PHIP pumped RASER and the route to chaos. Journal of Magnetic Resonance, 2021, 322, 106815.	1.2	19
124	PHIP hyperpolarized [1-13C]pyruvate and [1-13C]acetate esters via PH-INEPT polarization transfer monitored by 13C NMR and MRI. Scientific Reports, 2021, 11, 5646.	1.6	19
125	Efficient Synthesis of Molecular Precursors for Paraâ€Hydrogenâ€Induced Polarization of Ethyl Acetateâ€Iâ€ ¹³ C and Beyond. Angewandte Chemie, 2016, 128, 6175-6178.	1.6	18
126	Extending the Lifetime of Hyperpolarized Propane Gas through Reversible Dissolution. Journal of Physical Chemistry C, 2017, 121, 4481-4487.	1.5	18

#	Article	IF	CITATIONS
127	15 N Hyperpolarization of Dalfampridine at Natural Abundance for Magnetic Resonance Imaging. Chemistry - A European Journal, 2019, 25, 12694-12697.	1.7	18
128	Relaxation Dynamics of Nuclear Long-Lived Spin States in Propane and Propane-d6 Hyperpolarized by Parahydrogen. Journal of Physical Chemistry C, 2019, 123, 11734-11744.	1.5	18
129	A Versatile Compact Parahydrogen Membrane Reactor. ChemPhysChem, 2021, 22, 2526-2534.	1.0	17
130	"Direct―13 C Hyperpolarization of 13 Câ€Acetate by MicroTesla NMR Signal Amplification by Reversible Exchange (SABRE). Angewandte Chemie, 2020, 132, 426-431.	1.6	16
131	XeUS: A second-generation automated open-source batch-mode clinical-scale hyperpolarizer. Journal of Magnetic Resonance, 2020, 319, 106813.	1.2	16
132	Automated pneumatic shuttle for magnetic field cycling and parahydrogen hyperpolarized multidimensional NMR. Journal of Magnetic Resonance, 2020, 312, 106700.	1.2	16
133	High-Pressure Clinical-Scale 87% Parahydrogen Generator. Analytical Chemistry, 2020, 92, 15280-15284.	3.2	16
134	Relayed nuclear Overhauser enhancement sensitivity to membrane Cho phospholipids. Magnetic Resonance in Medicine, 2020, 84, 1961-1976.	1.9	16
135	Noninvasive Measurements of Glycogen in Perfused Mouse Livers Using Chemical Exchange Saturation Transfer NMR and Comparison to ¹³ C NMR Spectroscopy. Analytical Chemistry, 2015, 87, 5824-5830.	3.2	15
136	Parahydrogenâ€Induced Radio Amplification by Stimulated Emission of Radiation. Angewandte Chemie, 2020, 132, 8732-8738.	1.6	14
137	Cyclopropane Hydrogenation vs Isomerization over Pt and Pt–Sn Intermetallic Nanoparticle Catalysts: A Parahydrogen Spin-Labeling Study. Journal of Physical Chemistry C, 2020, 124, 8304-8309.	1.5	14
138	Efficient Batchâ€Mode Parahydrogenâ€Induced Polarization of Propane. ChemPhysChem, 2016, 17, 3395-3398.	1.0	13
139	Toward Cleavable Metabolic/pH Sensing "Double Agents―Hyperpolarized by NMR Signal Amplification by Reversible Exchange. Chemistry - A European Journal, 2018, 24, 10641-10645.	1.7	13
140	Magnetic shielding of parahydrogen hyperpolarization experiments for the masses. Magnetic Resonance in Chemistry, 2021, 59, 1180-1186.	1.1	13
141	Effects of Deuteration of ¹³ C-Enriched Phospholactate on Efficiency of Parahydrogen-Induced Polarization by Magnetic Field Cycling. Journal of Physical Chemistry C, 2018, 122, 24740-24749.	1.5	12
142	Heterogeneous hydrogenation of phenylalkynes with parahydrogen: hyperpolarization, reaction selectivity, and kinetics. Physical Chemistry Chemical Physics, 2019, 21, 26477-26482.	1.3	12
143	High Xe density, high photon flux, stopped-flow spin-exchange optical pumping: Simulations versus experiments. Journal of Magnetic Resonance, 2020, 312, 106686.	1.2	12
144	Heterogeneous Parahydrogenâ€Induced Polarization of Diethyl Ether for Magnetic Resonance Imaging Applications. Chemistry - A European Journal, 2021, 27, 1316-1322.	1.7	12

#	Article	IF	CITATIONS
145	Backgroundâ€Free Proton NMR Spectroscopy with Radiofrequency Amplification by Stimulated Emission Radiation. Angewandte Chemie - International Edition, 2021, 60, 26298-26302.	7.2	12
146	RASER MRI: Magnetic resonance images formed spontaneously exploiting cooperative nonlinear interaction. Science Advances, 2022, 8, .	4.7	12
147	Parahydrogenâ€Induced Polarization of Diethyl Ether Anesthetic. Chemistry - A European Journal, 2020, 26, 13621-13626.	1.7	11
148	Toward C13 hyperpolarized biomarkers produced by thermal mixing with hyperpolarized X129e. Journal of Chemical Physics, 2009, 131, 044508.	1.2	10
149	Synthetic approach for unsaturated precursors for parahydrogen induced polarization of choline and its analogs. Journal of Labelled Compounds and Radiopharmaceuticals, 2013, 56, 655-662.	0.5	9
150	Toward hyperpolarized molecular imaging of HIV: synthesis and longitudinal relaxation properties of ¹⁵ Nâ€Azidothymidine. Journal of Labelled Compounds and Radiopharmaceuticals, 2014, 57, 621-624.	0.5	9
151	Pilot multi-site quality assurance study of batch-mode clinical-scale automated xenon-129 hyperpolarizers. Journal of Magnetic Resonance, 2020, 316, 106755.	1.2	9
152	Synthetic Approaches for ¹⁵ N‣abeled Hyperpolarized Heterocyclic Molecular Imaging Agents for ¹⁵ N NMR Signal Amplification by Reversible Exchange in Microtesla Magnetic Fields. Chemistry - A European Journal, 2021, 27, 9727-9736.	1.7	9
153	Heterogeneous ¹ H and ¹³ C Parahydrogenâ€Induced Polarization of Acetate and Pyruvate Esters. ChemPhysChem, 2021, 22, 1389-1396.	1.0	9
154	Lowâ€Flammable Parahydrogenâ€Polarized MRI Contrast Agents. Chemistry - A European Journal, 2021, 27, 2774-2781.	1.7	8
155	High field <i>para</i> hydrogen induced polarization of succinate and phospholactate. Physical Chemistry Chemical Physics, 2021, 23, 2320-2330.	1.3	8
156	Synthesis and 15 N NMR Signal Amplification by Reversible Exchange of [15 N]Dalfampridine at Microtesla Magnetic Fields. ChemPhysChem, 2021, 22, 960-967.	1.0	8
157	Hyperpolarization of common antifungal agents with SABRE. Magnetic Resonance in Chemistry, 2021, 59, 1225-1235.	1.1	8
158	Scanning Nuclear Spin Level Anticrossings by Constant-Adiabaticity Magnetic Field Sweeping of Parahydrogen-Induced ¹³ C Polarization. Journal of Physical Chemistry Letters, 2022, 13, 1925-1930.	2.1	8
159	A versatile synthetic route to the preparation of ¹⁵ N heterocycles. Journal of Labelled Compounds and Radiopharmaceuticals, 2019, 62, 892-902.	0.5	7
160	Helium-rich mixtures for improved batch-mode clinical-scale spin-exchange optical pumping of Xenon-129. Journal of Magnetic Resonance, 2020, 315, 106739.	1.2	6
161	¹⁵ N NMR Hyperpolarization of Radiosensitizing Antibiotic Nimorazole by Reversible Parahydrogen Exchange in Microtesla Magnetic Fields. Angewandte Chemie, 2021, 133, 2436-2443.	1.6	6
162	Gas-Phase NMR of Hyperpolarized Propane with 1H-to-13C Polarization Transfer by PH-INEPT. Applied Magnetic Resonance, 2022, 53, 653-669.	0.6	6

#	Article	IF	CITATIONS
163	New aspects of parahydrogen-induced polarization for C2—C3 hydrocarbons using metal complexes. Russian Chemical Bulletin, 2021, 70, 2382-2389.	0.4	4
164	Parahydrogen-Induced Magnetization of Jovian Planets?. ACS Earth and Space Chemistry, 2020, 4, 495-498.	1.2	3
165	Automated Low-Cost In Situ IR and NMR Spectroscopy Characterization of Clinical-Scale 129Xe Spin-Exchange Optical Pumping. Analytical Chemistry, 2021, 93, 3883-3888.	3.2	3
166	Bridging the Gap: From Homogeneous to Heterogeneous Parahydrogenâ€induced Hyperpolarization and Beyond. ChemPhysChem, 2021, 22, 710-715.	1.0	3
167	Enabling Clinical Technologies for Hyperpolarized ¹²⁹ Xenon Magnetic Resonance Imaging and Spectroscopy. Angewandte Chemie, 2021, 133, 22298-22319.	1.6	3
168	Pilot Quality-Assurance Study of a Third-Generation Batch-Mode Clinical-Scale Automated Xenon-129 Hyperpolarizer. Molecules, 2022, 27, 1327.	1.7	3
169	Frontispiece: NMR Hyperpolarization Techniques of Gases. Chemistry - A European Journal, 2017, 23, .	1.7	2
170	Backgroundâ€Free Proton NMR Spectroscopy with Radiofrequency Amplification by Stimulated Emission Radiation. Angewandte Chemie, 0, , .	1.6	2
171	Highâ€Resolution 3D Proton MRI of Hyperpolarized Gas Enabled by Parahydrogen and Rh/TiO ₂ Heterogeneous Catalyst. Chemistry - A European Journal, 2014, 20, 11597-11597.	1.7	1
172	NMR Hyperpolarization Techniques of Gases. Chemistry - A European Journal, 2017, 23, 724-724.	1.7	1
173	Unique Insights into the Structural and Functional Biology of Membrane Proteins from Solid State NMR Spectroscopy. Biophysical Journal, 2018, 114, 207a.	0.2	1
174	NMR Spectroscopy Techniques: Hyperpolarization for Sensitivity Enhancement. , 2018, , 168-168.		1
175	Limits of Spatial Resolution of Phase Encoding Dimensions in MRI of Metals. Journal of Physical Chemistry Letters, 2019, 10, 375-379.	2.1	1
176	Parawasserstoffâ€induzierte Hyperpolarisation von Gasen. Angewandte Chemie, 2020, 132, 17940-17949.	1.6	1
177	Anisotropie Chemical Shift Perturbation Induced by Ions in Conducting Channels. , 2008, , 279-283.		Ο
178	Sodium 3D COncentration MApping (COMA 3D) using 23Na and proton MRI. Journal of Magnetic Resonance, 2014, 247, 88-95.	1.2	0
179	Gramicidin Ion Binding and Conductance: New Insights from 170 Solid State NMR Spectroscopy in a 1.5 GHZ Spectrometer. Biophysical Journal, 2018, 114, 305a-306a.	0.2	0
180	NMR for Biological Systems. ChemPhysChem, 2019, 20, 177-177.	1.0	0

#	Article	IF	CITATIONS
181	Frontispiece: Parahydrogenâ€Induced Polarization of Diethyl Ether Anesthetic. Chemistry - A European Journal, 2020, 26, .	1.7	0
182	Frontispiece: Heterogeneous Parahydrogenâ€Induced Polarization of Diethyl Ether for Magnetic Resonance Imaging Applications. Chemistry - A European Journal, 2021, 27, .	1.7	0
183	Frontispiece: Synthetic Approaches for ¹⁵ N‣abeled Hyperpolarized Heterocyclic Molecular Imaging Agents for ¹⁵ N NMR Signal Amplification by Reversible Exchange in Microtesla Magnetic Fields. Chemistry - A European Journal, 2021, 27, .	1.7	0
184	Innentitelbild: Backgroundâ€Free Proton NMR Spectroscopy with Radiofrequency Amplification by Stimulated Emission Radiation (Angew. Chem. 50/2021). Angewandte Chemie, 2021, 133, 26206-26206.	1.6	0